Optimization of process parameters for friction stir processing (FSP) of Al–TiC *in situ* composite

RANJIT BAURI*

Department of Metallurgical and Materials Engineering, Indian Institute of Technology Madras,
Chennai 600 036, India

Abstract. Segregation of *in situ* formed particles at the grain boundaries is a major drawback of *in situ* composites. In this study, it has been demonstrated that friction stir processing (FSP) can be used as an effective tool to homogenize the particle distribution in Al based *in situ* composites and FSP processing parameters were optimized for this purpose. An Al-5 wt% TiC composite was processed *in situ* using K_2TiF_6 and graphite in Al melt and subjected to FSP. Processing parameters for FSP were optimized to get a defect free stir zone and homogenize the particle distribution. It was found that a rotation speed > 800 rpm is needed. A rotation speed of 1000 rpm and a traverse speed of 60 mm/min were found to be an optimum combination. The grain size was also refined in addition to homogenization of the as-cast microstructure. This resulted in significant improvement in the mechanical properties of the processed composite.

Keywords. *In situ* composites; friction stir processing; microstructure; grain refinement; mechanical properties.

1. Introduction

Discontinuously reinforced aluminum matrix composites (DRAMCs) have been the subject of interest and extensive research in the field of metal matrix composites (MMCs) owing to their improved properties such as high specific strength and stiffness (Arsenault *et al* 1991; Lloyd 1994; Gupta and Surappa 1995), superior wear resistance (Pramila Bai *et al* 1992). Several processing routes have been employed to make such composites. Liquid metallurgy or stir casting route is one of the most commonly used methods. In this technique, reinforcement particles are introduced to the liquid metal externally through mechanical agitation of the melt. Powder metallurgy is another technique which has been employed extensively to process these composites. The major drawbacks of these processes are inhomogeneous distribution (clustering) and improper wetting of particles which lead to poor mechanical properties. Therefore, *in situ* processes, wherein the reinforcements are formed during processing itself have been adapted as a strategy to overcome these problems (Shtessel *et al* 1994; Premkumar and Chu 1995; Chen and Chung 1996). The resultant *in situ* composites are found to exhibit better properties due to improved wettability of particles, a clean particle-matrix interface and strong bonds between the reinforcement and metallic matrix (Sahoo and Koczak 1991; Koczak and Premkumar 1993; Fan *et al* 1994). Al–TiC composites have attracted increasing attention amongst the *in situ* composites due to the attractive properties of TiC as reinforcement such as high elastic modulus and hardness. Furthermore, TiC particles also refine the grain size by providing nucleation sites during solidification (Mohanty and Gruzleski 1994; Vinod Kumar *et al* 2005; Prasad Rao *et al* 2009). However, a major disadvantage of these *in situ* composites is the tendency of the particles to segregate along the grain boundaries and it is difficult to avoid this segregation during processing (Tong and Fang 1998; Ding *et al* 2007; Birol 2008). Several approaches such as isothermal holding above the melting point for prolonged period, extrusion, rolling have been explored to break the grain boundary agglomerates and improve the distribution of *in situ* particles (Tee *et al* 1999a, b; Feng and Froyen 2000; Kerti 2005; Watson *et al* 2005; Herbert *et al* 2007). However, once formed, it was difficult to break the large agglomerates of particles by such processes. Moreover, there are chances of failures if a secondary process like rolling is employed to improve particle distribution (Herbert *et al* 2007).

Therefore, it is imperative to develop methods which can effectively improve the particle distribution in *in situ* metal matrix composites. Friction stir processing (FSP) has been emerging as a generic tool for material processing and microstructure modification (Berbon *et al* 2001;

*Author for correspondence (rbauri@iitm.ac.in)

Mishra and Ma 2005; Ma *et al* 2006; Su *et al* 2006). FSP uses a rotating cylindrical tool having a shoulder and pin which is pressed against the material to be processed and traversed at a particular speed for a desired length. The side in which the tangential velocity of the tool surface is parallel to the traverse direction is defined as the advancing side and the antiparallel one is defined as the retreating side. The local heating due to friction and forging action of the tool deform and process the material at an elevated temperature below its melting point. Since, it involves significant material flow at elevated temperatures, the process also offers the possibility of redistributing the particles in metal matrix composites (Bauri *et al* 2011a, b). However, right processes parameters are needed to be evolved to serve this purpose.

The aim of the present study is to improve the homogeneity of particle distribution in Al–TiC *in situ* composites and establish FSP processing window to serve this purpose and to obtain a defect free stir zone by optimizing the process parameters, viz. rotation and traverse speeds of the tool. The effect of FSP on the microstructure and mechanical properties has been evaluated.

2. Experimental

2.1 *Composite fabrication*

K_2TiF_6 salt (CDH, India) and graphite powder (Lobachemie, India) of average particle size 50 μm was used as the source of Ti and C respectively to form TiC particles *in situ* in the aluminum melt. Required amounts of K_2TiF_6 salt and graphite powders corresponding to 5 wt% of TiC were taken and mixed thoroughly. A slightly more graphite powder than the stoichiometric amount was taken to compensate for the oxidation losses during processing. The mixture was wrapped in aluminum foils into number of capsules and pre-heated at around 200 °C to drive away the moisture. Commercially pure Al was melted in a resistance-heated furnace under argon atmosphere. The temperature of the melt was monitored with the help of a thermocouple. When the temperature reached to 1200 °C, K_2TiF_6 and graphite mixture was added and the melt was held for 1 h to complete the reaction. The details of the process for arriving at the optimum processing parameters to form TiC particles *in situ* are described by Bauri (2009). The melt was stirred intermittently with a stirring rod to disperse the *in situ* formed particles. Finally, the spent salt was decanted before pouring and the melt was cast in pre-heated cast irons moulds in the form of a plate.

2.2 *Friction stir processing*

The as-cast composite plate was machined to a thickness of 10 mm for friction stir processing (FSP). The tool used to carry out FSP is made of M2 tool steel and consists of a shoulder of diameter 12 mm and a pin of 4 mm in diameter. The pin length was 3·5 mm. FSP parameters, rotation and traverse speeds were optimized by trying out several combinations on separate tracks which are shown in figure 1. The vertical force and the plunge depth are predefined and were fixed at 5 kN and 4·2 mm, respectively. The stir zone was inspected visually and under SEM for each combination to establish the right process parameters for a defect free stir zone. Table 1 shows all the parameters used in the experiments.
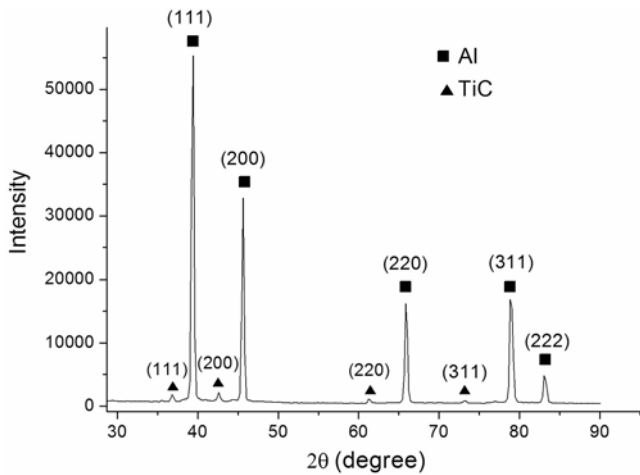
2.3 *Characterization*

Samples were sliced from the as-cast and stir zone of the plate for microstructural investigations. For optical and scanning electron microscopy (SEM), samples were polished with emery paper up to 1200 grit followed by polishing with alumina suspension and 1 μm diamond paste to give a mirror finish. For electron backscattered diffraction (EBSD) studies, samples were electro-polished using a mixture of perchloric acid and methanol at −12 °C and observations were made at 30 kV in a FEI Quanta FEG SEM equipped with a TSL–OIM software. Samples for transmission electron microscopy (TEM), were cut from the stir zone and were carefully polished to a thickness of 90 μm and subjected to twin-jet polishing using a mixture of 20% perchloric acid and methanol at −20 °C. Observations
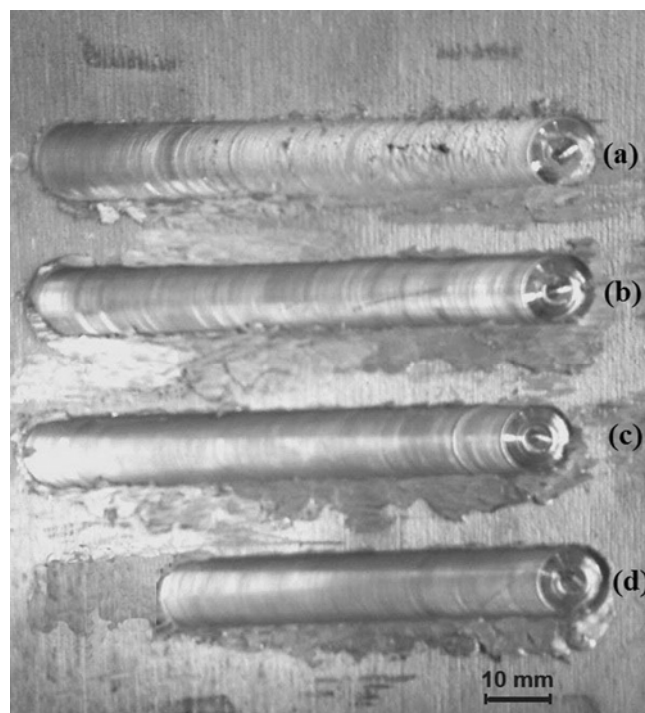
Figure 1. Macrograph of FSP tracks (a) 640 rpm, 60 mm/min, (b) 800 rpm, 60 mm/min, (c) 800 rpm, 120 mm/min and (d) 800 rpm, 150 mm/min.

Table 1. FSP process parameters.

Experiment no.	Rotation speed (rpm)	Traverse speed (mm/min)	Vertical force (kN)	Plunge depth (mm)
1	640	60	5	4·2
2	800	60	5	4·2
3	800	120	5	4·2
4	800	150	5	4·2
5	1000	60	5	4·2

Figure 2. XRD pattern of Al–TiC *in situ* composite.

were made in a Philips CM-20 TEM operating at 200 kV. X-ray diffraction was carried out in a Brukers D8 diffractometer using CuKα radiation ($\lambda = 0.154$ nm) for phase analysis.

2.4 *Mechanical property evaluation*

Mechanical properties were evaluated by hardness and tensile tests. Vickers microhardness tests were carried out using a Wolpert–Wilson microhardness tester with a load of 100 g and a dwell time of 20 s. Tensile specimens of 1 mm thickness and 10 mm gauge length were sliced from the stir zone parallel to the tool traverse direction by electrical discharge machining (EDM) and tests were carried out as per ASTM standard on an Instron machine (Model 3367) at a strain rate of 10^{-3} s^{-1}.

3. Results and discussion

3.1 *XRD phase analysis*

Ti has very little solubility in Al and hence, readily forms Al$_3$Ti intermetallics which are brittle in nature and deteriorate the properties. Therefore, the processing parameters were controlled carefully in Al melt during the processing of Al–TiC *in situ* composites to avoid formation of the intermetallics. X-ray diffraction analysis was

performed to verify that no such undesirable intermetallic is present in the composite. XRD pattern in figure 2 shows that peaks corresponding to only Al and TiC are present and no peaks belonging to Al$_3$Ti or any other undesirable phase was found in the as-cast Al–TiC composite.

3.2 *Optimization of FSP process parameters*

The first FSP pass was carried out with a tool rotation speed of 640 rpm and traverse speed of 60 mm/min as these were found suitable for processing the pure Al matrix (Yadav and Bauri 2011a, b). The stir zone exhibited too many defects as shown in figure 1 (track a). Hence, a rotation speed of 640 rpm was not sufficient to process the composite. Therefore, the rotation speed was increased to 800 rpm in the next experiment and the traverse speed was kept constant at 60 mm/min (table 1). In this case, though a smooth stir zone was observed visually (figure 1, track b), however, when it was observed under SEM large defects running parallel to the stir zone were found as shown in figure 3(a). Since increasing the rotation speed suppressed the formation of macro defects and gave a good surface finish, it was logical to vary the traverse speed at the same rotational speed (800 rpm) in the next experiment. Hence, the next set of FSP experiments were carried out at 800 rpm, one with a traverse speed of 120 mm/min and the other with a traverse speed of 150 mm/min. However, the observations in these cases were same as the previous one (800 rpm and 60 mm/min), i.e., good surface finish (tracks c and d) but presence of defects revealed by SEM (figures 3b and c). The particle distribution was also not improved as clusters of TiC particles at grain boundaries were still observed (figure 3d). Therefore, it was clear that even a rotational speed of 800 rpm was not sufficient to process the composite and the effect of traverse speed was not very significant. The amount of heat input into the material during FSP depends on the ratio of tool rotation to traverse speed. Higher the ratio higher is the heat input. A minimum ratio of tool rotation to traverse speed is needed for a given material below which, the heat produced by friction and stirring may not be sufficient to soften and plasticise the material, and it may not flow around the rotating tool to produce a continuous defect free stir zone.
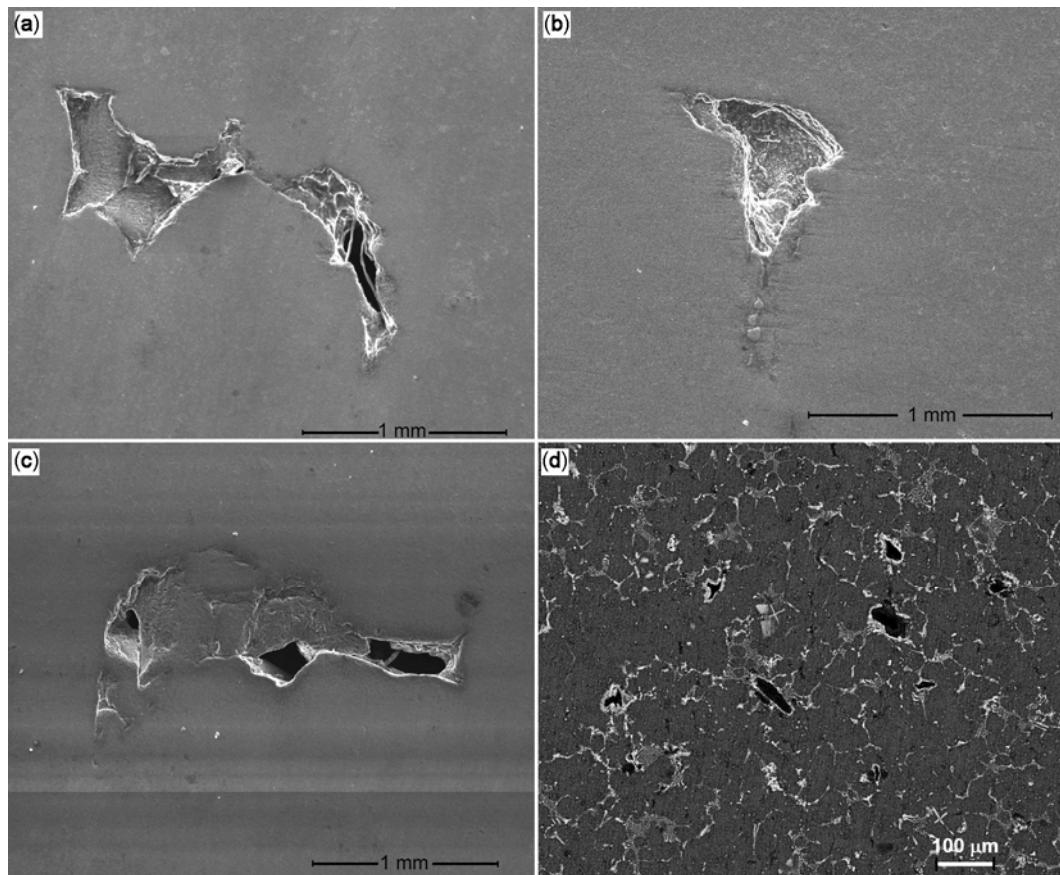
Figure 3. SEM images of 800 rpm sample showing defects (**a**) traverse speed of 60 mm/min, (**b**) 120 mm/min and (**c**) 150 mm/min. (**d**) Particle clusters at grain boundaries after FSP.
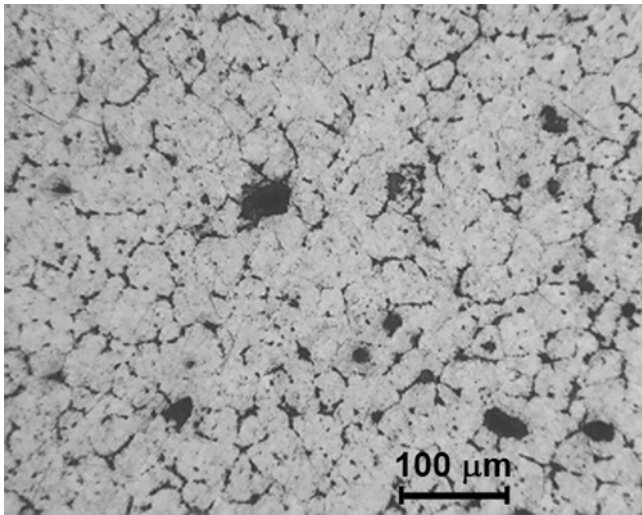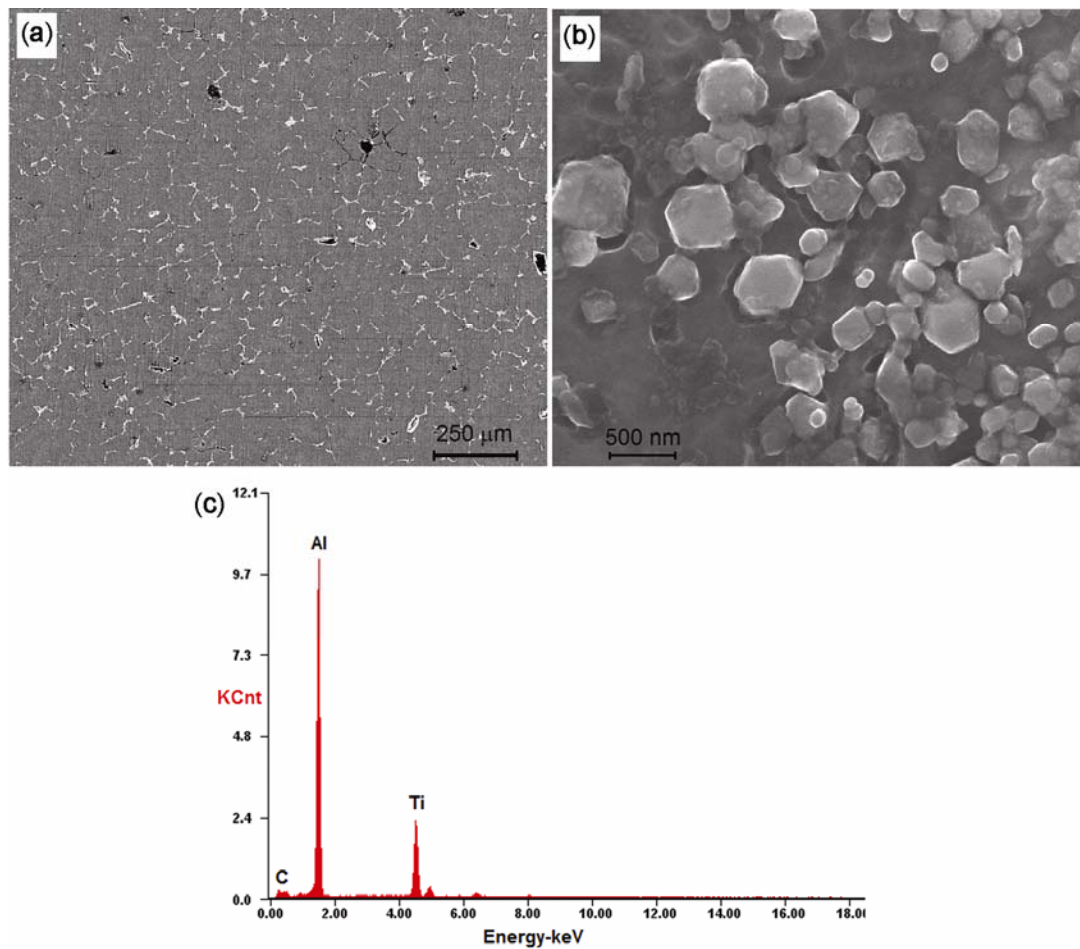

Figure 4. Optical micrograph of as-cast Al–TiC composite.

Hence, a rotational speed of 1000 rpm with traverse speed of 60 mm/min was used finally to process the composite. The composite processed with these parameters exhibited a defect free stir zone and the particle distribution also improved as described in next section.

3.3 *Microstructure*

An optical micrograph of the as-cast Al–TiC composite is shown in figure 4. It can be seen that TiC particles delineate the grain boundaries as they are segregated along the boundaries. SEM micrograph in figure 5(a) shows similar features. One such grain boundary cluster is shown in the higher magnification SEM image in figure 5(b). The size and morphology of the particles can be clearly seen from this figure. Most of the TiC particles are sub-micron in size and many ultrafine particles were also observed. An EDS taken on one such particle confirms these to be TiC (figure 5c).

The distribution of particles in MMC depends on whether the solidification front is engulfing (uniform distribution) or pushing (clustering) the particles. The engulfment or pushing of particles is influenced by the shape of the solid–liquid interface that approaches the particles during solidification. The solid–liquid interface is assumed to follow the isotherms of the melting point of the matrix material. The nature of the temperature isotherms depends on the ratio of thermal conductivities of the particles and the matrix, $\alpha = k_p/k_m$ (k_p and k_m are thermal conductivity of particles and matrix respectively). For $\alpha = 1$, the isotherms are uniform (planar

Figure 5. (**a**) SEM micrograph of as-cast Al–TiC composite showing particle segregation at grain boundaries, (**b**) high magnification image showing a particle cluster and (**c**) EDS taken on a particle.
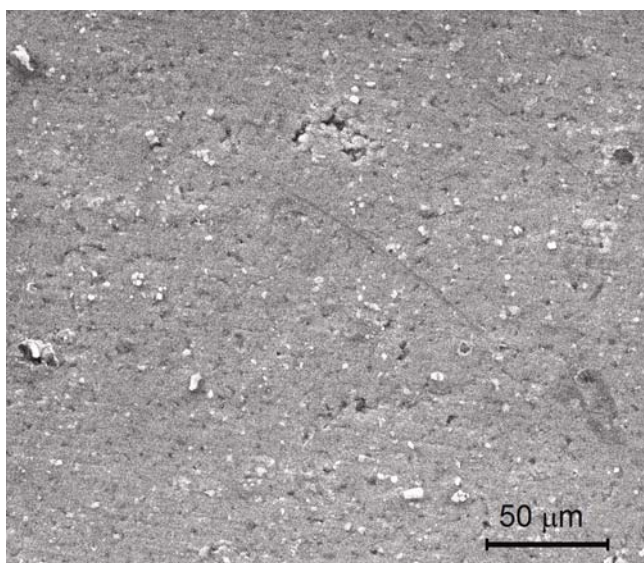
Figure 6. SEM micrograph of Al–TiC composite friction stir processed at 1000 rpm and 60 mm/min showing uniform distribution of TiC particles (white particles).

interface), but get deflected near the particle, if α differs from unity. For $\alpha > 1$ the isotherms converge (concave) towards the particles, i.e. a trough is developed on the interface behind the particles leading to their engulfment (Shangguan *et al* 1992). On the other hand, if $\alpha < 1$ the isotherms diverge from the particles (convex) and a bump is developed on the interface behind the particle and pushing is expected to occur as the particles will roll down the bump.

The forces acting on the particles in the melt also affect their distribution in the matrix. A general description of these forces and their effect on the particle distribution in MMCs is given by Shangguan *et al* (1992). There are three types of forces acting on a particle; (i) the gravitational force F_g, (ii) the force due to interfacial energy F_i and (iii) the drag force due to flow around the particle F_d.

Generally, a lighter particle is pushed by the solidification front as F_g will act upwards. The interfacial force depends on the value of α and hence, affects the particle distribution the same way as α does. The drag force F_d, that arises due to the relative velocity of the particles with

respect to the melt is always conducive for particle engulfment.

It has been also reported that a critical velocity of the solidification front decides the engulfment to pushing transition (Van Vugt and Froyen 1997; Stefanescu *et al* 1998). Below the critical velocity, the particles are pushed by the solidification front resulting in their segregation in the inter-dendritic regions on solidification. Above the critical velocity, the front grows around the particles and engulfs them leading to distribution in the grains.
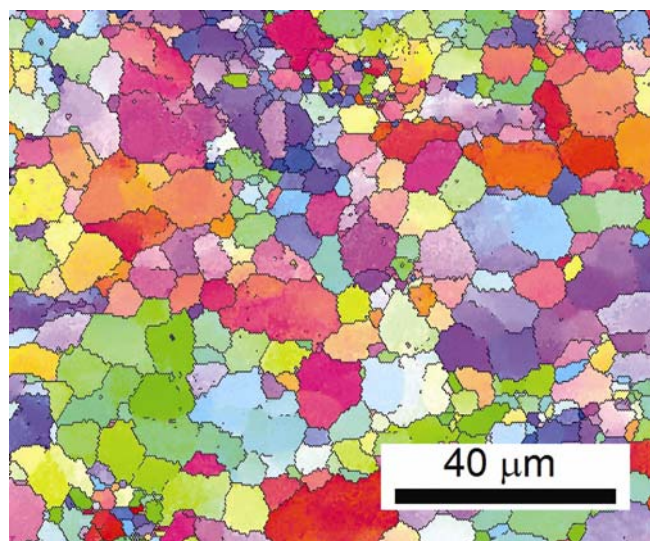
TiC particles in the present case, therefore, seem to be pushed by the solidification front leading to their segregation in the inter-dendritic regions (grain boundaries).

The objective of carrying out friction stir processing (FSP) on the as-cast composite was to improve the homogeneity of particle distribution. SEM micrograph in figure 6 shows microstructure of the composite after a single FSP pass at 1000 rpm and 60 mm/min. It can be seen that the particle clusters are broken from the grain boundaries and distributed in the matrix (grain interiors) leading to improved homogeneity. The primary attribute to this can be given to the material flow around the tool during FSP. The tool rotates and then moves ahead leaving behind a plastic deformed material. The side in which the tangential velocity of the tool surface is parallel to the traverse direction is defined as the advancing side and the other side is the retreating side. The material flows from the retreating side to the advancing side and as the tool moves ahead in the advancing side, the deformed materials is deposited behind the tool on the retreating side. The material is thus pushed downward on the advancing side and moves upward on the retreating side within the pin diameter. This severe plastic flow that imparts both forging and extrusion actions on the material facilitates

movement of the particles leading to their homogeneous distribution.

In addition to homogenizing the particle distribution, FSP of the composite also refined the grain size and eliminated most of the casting defects. EBSD image (IPF + grain boundary map) in figure 7 shows a recrystallized fine-grained structure. The average grain size was found to be 9 μm as compared to 48 μm for the as-cast material. It has been shown that dynamic recrystallization (DRX) occurs during FSP (Jata and Semiatin 2004; Su *et al* 2005; Yadav and Bauri 2011) as the thermomechanical aspect of the process provides enough driving force for occurrence of dynamic recovery (DRV) that precedes DRX leading to an equi-axed fine grain structure. The microstructure evolution is further discussed below with the aid of transmission electron microscopy (TEM) investigation.

TEM micrograph in figure 8(a) shows fine equiaxed grains in the friction stir processed (FSPed) composite. Distribution of fine TiC particles inside a grain can be seen in figure 8(b). Dislocations are generated during plastic deformation in FSP. The mismatch in thermal expansion coefficient between the particles and the matrix and their differential deformation behaviour also generates additional dislocations during FSP. A high dislocation density can be observed inside the grains in figure 8(c). Dislocations arrange themselves into low-angle subgrain boundaries through dynamic recovery (DRV) which occurs readily in aluminum due to its high stacking fault energy (~ 200 mJ/m^2). TEM micrograph in figure 8(d) shows a recovery structure. The sub-grains thus formed act as nuclei for the dynamic recrystallization process that happens subsequently during FSP leading to the fine-grained structure.

3.4 *Mechanical properties*

The effect of FSP on the mechanical properties was evaluated by hardness and tensile tests. Vickers microhardness was measured as a function of distance from the centre of the stir zone on either side (advancing and retreating). The hardness profile is shown in figure 9. The hardness of the FSPed composite improved significantly compared to that of the as-cast composite. The average hardness of the FSPed composite was 48 Hv compared to 38 Hv for the as-cast composite (shown by the straight horizontal line in figure 9). However, the hardness profile across the stir zone (the central upper part, up to 6 mm on either side in figure 9) shows some fluctuations. The material flows in a complex fashion from the retreating to the advancing side during FSW/FSP (Mishra and Ma 2005) giving rise to gradients in temperature, strain and strain rate across the stir zone. This in turn gives rise to different microstructural features at different locations in the stir zone (Yutaka *et al* 2001; Yadav and Bauri 2011a, b)

Figure 7. EBSD image of friction stir processed Al–TiC composite.

Table 2. Mechanical properties of as-cast and processed Al–TiC composites.

Materials	Hardness $(HV_{0.1})$	0·2% Proof stress (MPa)	UTS (MPa)	% Elongation
As-cast Al–TiC	38	88	137	15·7
FSPed Al–TiC	48	103	163	16
Al–5% TiC (Jerome *et al* 2010)	–	–	127	9
Al–5% TiB$_2$ (Tee *et al* 1999a, b)	–	96	124	9·2
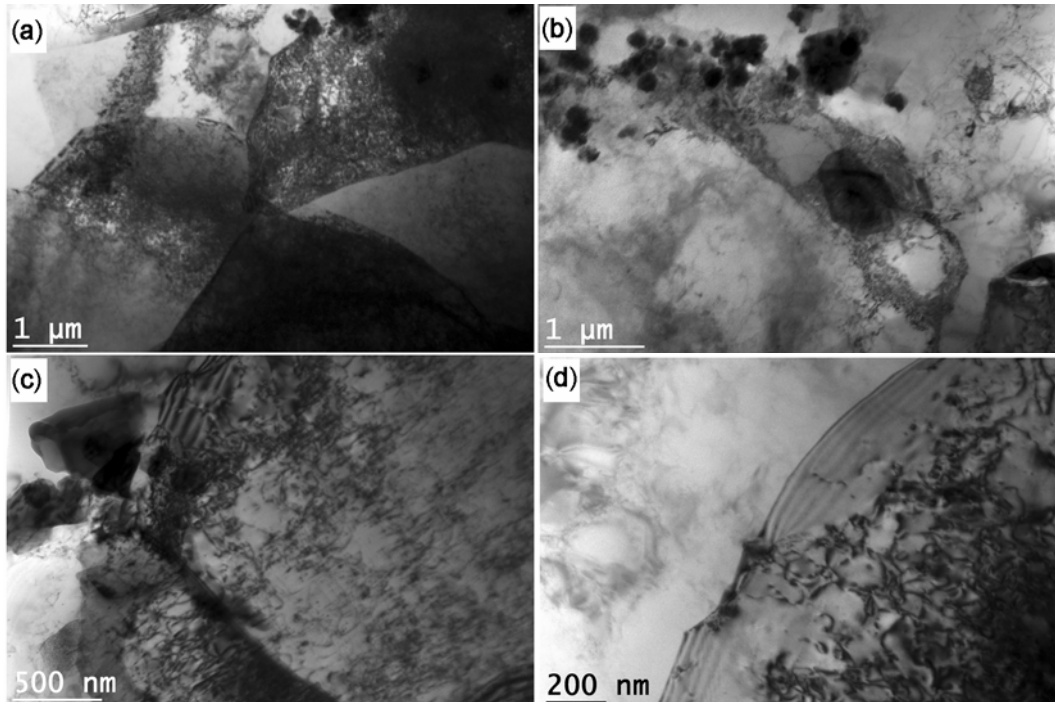
Figure 8. TEM micrographs of FSPed composite showing (**a**) equiaxed fine grains, (**b**) TiC particles inside grains, (**c**) high dislocation density and (**d**) recovery structure.
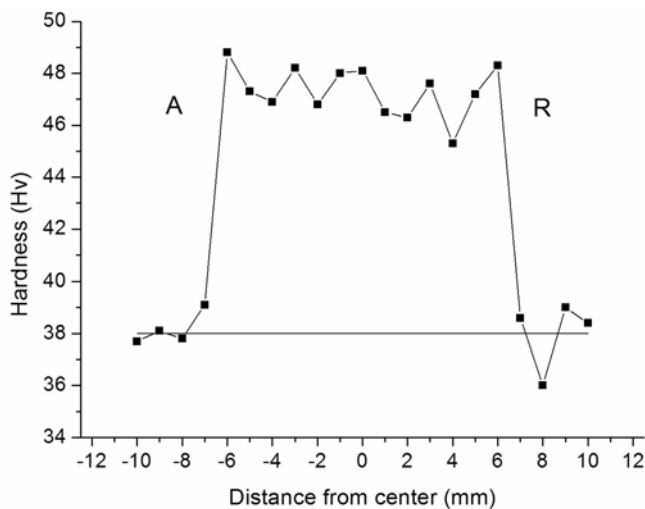
Figure 9. Hardness profile of stir zone of Al–TiC composite (advancing and retreating sides are marked as A and R, respectively).

resulting in some variation in the hardness within the stir zone.

The tensile properties of the FSPed composite also improved substantially compared to the as-cast composite. 0·2% proof stress after FSP increased by 17% to 103 MPa compared to 88 MPa of the as-cast composite. UTS of the processed composite (163 MPa) also increased significantly compared to the as-cast composite (137 MPa). This can be attributed to the improved microstructure due to FSP. One of the prominent mechanisms of strengthening in MMCs is the hindrance to dislocation motion by the reinforcing particles. As the particle distribution improves after FSP, the dislocation hindrance mechanism becomes more effective and the strength is enhanced. The higher dislocation density (due to additional dislocation generation as stated above) further increases the resistance to dislocation motion and hence, increases the strength. The grain size refinement also contributes to the strengthening. In case of MMCs, the improvement in

strength is invariably associated with the significant reduction in ductility. However, in the present case one noble aspect of the processed Al–TiC composite is that the ductility was not compromised for the increase in the strength. Though a better ductility is expected due to the achieved grain refinement, the strength-ductility combination was still a lot better compared to conventional or even similar *in situ* composites as shown by comparison with the literature data in table 2 which summarizes the hardness and tensile properties.

4. Conclusions

Friction stir processing (FSP) was employed to improve the homogeneity of particle distribution in Al–TiC *in situ* composite. The processing parameters for friction stir processing of the composite were optimized and a defect free stir zone with improved microstructure was obtained. Following conclusions can be drawn from this study.

(I) A rotation speed of > 800 rpm was needed to obtain a defect free stir zone on Al–TiC composite. A rotation speed of 1000 rpm and traverse speed of 60 mm/min were found to be an optimum combination.

(II) Friction stir processing homogenized the microstructure of Al–TiC *in situ* composite and refined the grain size.

(III) TEM and EBSD studies revealed a dynamically recrystallized equiaxed grain structure after FSP.

(IV) The mechanical properties improved significantly after FSP compared to the as-cast composite.

References

Arsenault R J, Wang L and Feng C R 1991 *Acta Meta. Mater.* **39** 47

Bauri R 2009 *Trans. IIM* **62** 391

Bauri R, Yadav D and Suhas G 2011 *Mater. Sci. Eng.* **A528** 4732

Berbon P B, Bingel W H, Mishra R S, Bampton C C and Mahoney M W 2001 *Scr. Mater.* **44** 61

Birol Y 2008 *J. Alloys Compd.* **454** 110

Chen Y and Chung D D L 1996 *J. Mater. Sci.* **31** 311

Ding H, Liu X, Yua L and Zhao G 2007 *Scr. Mater.* **57** 575

Fan Z, Miodownik A P, Chandrasekaran L and Ward-Close M 1994 *J. Mater. Sci.* **29** 1127

Feng C F and Froyen L 2000 *J. Mater. Sci.* **35** 837

Gupta M and Surappa M K 1995 *Key Eng. Mater.* **104–107** 259

Herbert M A, Sarkar C, Mitra R and Chakraborty M 2007 *Met. Mater. Trans.* **A38** 2110

Jata K V and Semiatin S L 2004 *Scr. Mater.* **43** 743

Jerome S, Ravisankar B, Mahato P K and Natarajan S 2010 *Trib. Int.* **43** 2029

Kerti I 2005 *Mater. Lett.* **59** 3795

Koczak M J and Premkumar M K 1993 *JOM* **45** 44

Lloyd D J 1994 *Int. Mater. Rev.* **39** 1

Ma Z Y, Sharma S R and Mishra R S 2006 *Mater. Sci. Eng.* **A433** 269

Mishra R S and Ma Z Y 2005 *Mater. Sci. Eng.* **R50** 1

Mohanty P S and Gruzleski J E 1994 *Scr. Met. Mater.* **31** 179

Pramila Bai B N, Ramashesh B S and Surappa M K 1992 *Wear* **157** 295

Prasada Rao A K, Das K, Murty B S and Chakraborty M 2009 *J. Alloys Compd.* **480** L49

Premkumar M K and Chu M G 1995 *Mater. Sci. Eng.* **A202** 172

Sahoo P and Koczak M J 1991 *Mater. Sci. Eng.* **A144** 37

Shangguan D, Ahuja S and Stefanescu D M 1992 *Met. Mater. Trans.* **A23** 669

Shtessel V, Sampath S and Koczak M 1994 *In situ composites: science and technology* (eds) M Singh and D Lewis (Warrendale, PA: The Minerals, Metals and Materials Society) p 37

Stefanescu D M, Dhindaw B K, Kacar S A and Moitra A 1998 *Meta. Trans.* **A19** 2847

Su J Q, Nelson T W and Sterling C J 2005 *Mater. Sci. Eng.* **A405** 277

Su J Q, Nelson T W and Sterling C J 2006 *Phil. Mag.* **86** 1

Tee K L, Lu L and Lai M O 1999a *Comp. Struc.* **47** 589

Tee K L, Lu L and Lai M O 1999b *J. Mater. Proc. Tech.* **89–90** 513

Tong X C and Fang H S 1998 *Met. Mater. Trans.* **A29** 875

Van Vugt L and Froyen L 1997 *Micrograv. Sci. Tech.* **10** 95

Vinod Kumar G S, Murty B S and Chakraborty M 2005 *J. Alloy Compd.* **396** 143

Watson I G, Forster M F, Lee P D, Dashwood R J, Hamilton R W and Chirazi A 2005 *Composites: Part A* **36** 1177

Yadav D and Bauri R 2011a *Mater. Sci. Tech.* **27** 1163

Yadav D and Bauri R 2011b *Mater. Sci. Eng.* **A528** 1326

Yutaka S S, Park S H C and Kokawa H 2001 *Meta. Mater. Trans.* **A32** 3033